Binding of Transducin and Transducin-Derived Peptides to Rhodopsin Studied by Attenuated Total Reflection–Fourier Transform Infrared Difference Spectroscopy

Karim Fahmy
Institut für Biophysik und Strahlenbiologie der Albert-Ludwigs-Universität Freiburg, 79104 Freiburg, Germany

ABSTRACT Fourier transform infrared difference spectroscopy combined with the attenuated total reflection technique allows the monitoring of the association of transducin with bovine photoreceptor membranes in the dark. Illumination causes infrared absorption changes linked to formation of the light-activated rhodopsin-transducin complex. In addition to the spectral changes normally associated with meta II formation, prominent absorption increases occur at 1735 cm^{-1}, 1640 cm^{-1}, 1550 cm^{-1}, and 1517 cm^{-1}. The D_2O sensitivity of the broad carbonyl stretching band around 1735 cm^{-1} indicates that a carboxylic acid group becomes protonated upon formation of the activated complex. Reconstitution of rhodopsin into phosphatidylcholine vesicles has little influence on the spectral properties of the rhodopsin-transducin complex, whereas pH affects the intensity of the carbonyl stretching band. A C-terminal peptide comprising amino acids 340–350 of the transducin α-subunit reproduces the frequencies and isotope sensitivities of several of the transducin-induced bands between 1500 and 1800 cm^{-1}, whereas an N-terminal peptide (aa 8–23) does not. Therefore, the transducin-induced absorption changes can be ascribed mainly to an interaction between the transducin-α C-terminus and rhodopsin. The 1735 cm^{-1} vibration is also seen in the complex with C-terminal peptides devoid of free carboxylic acid groups, indicating that the corresponding carbonyl group is located on rhodopsin.

INTRODUCTION

The seven helix photoreceptor rhodopsin has been studied intensively as a model for G protein-coupled receptors (Hargrave et al., 1993; Baldwin, 1994; Helmreich and Hofmann, 1996). The chromophore 11-*cis* retinal is attached to Lys^{296} of opsin by a protonated Schiff base linkage (Bownds, 1967; Oseroff and Callender, 1974; Hargrave and McDowell, 1992) and senses conformational changes in rhodopsin after photoisomerization to all-*trans* retinal. Thus intermediates of the photoactivation process can be defined by UV-visible spectroscopy (Yoshizawa and Wald, 1963; Lewis and Kliger, 1992). However, a molecular characterization of conformational changes is hard to extract from these data. Fourier transform infrared (FTIR) difference spectroscopy can monitor light-induced changes of molecular vibrational modes and has contributed substantially to our information on intramolecular changes in the photointermediates of rhodopsin (for a recent review see Siebert, 1995). Ultimately, these light-dependent alterations in the transmembrane region are transmitted to the cytoplasmic surface in the metarhodopsin II (MII) state, which catalyzes nucleotide exchange in transducin (Emeis et al., 1982; Kibelbek et al., 1991), the G protein of the photoreceptor cell (G_t). Although interaction sites have been identified (König et al., 1989a), the assignment of infrared absorption changes to specific groups on rhodopsin's surface has not reached the degree of specificity established for its transmembrane part. Moreover, the biologically relevant complex formation between light-activated rhodopsin and G_t has only recently been observed by transmissive FTIR difference spectroscopy (Nishimura et al., 1996). In principle, FTIR difference spectroscopy should be able to contribute to the understanding of intermolecular processes during protein-protein recognition with the same molecular resolution as has been achieved for intramolecular processes. However, with transmissive infrared spectroscopy, the study of protein-protein interactions has to be carried out in the absence of bulk water to reduce strong background infrared absorption. In addition, the sealed sample compartment prevents the addition of proteins or small ligands during spectral recordings. The latter is particularly desired when nucleotide-dependent receptor G protein coupling is studied. Here FTIR difference spectroscopy is combined with the attenuated total reflectance (ATR) method (Harrick, 1967) to study rhodopsin-G_t interactions. This method allows the application of infrared spectroscopy under conditions that resemble those encountered in the native system, i.e., the membrane-bound receptor can be investigated in binding equilibrium with G protein in a bulk water phase. Because of restriction of the evanescent field to a small volume at the surface of an internal reflection element (IRE), a sample compartment can be employed to which proteins or ligands can be added during the measurement. This allows one to obtain difference spectra from membrane proteins attached to an IRE in the presence or absence of soluble ligands by perfusing the IRE with appropriate solutions (Baenziger et al., 1993). In the present study, it is shown that dark association of G_t with photoreceptor membranes, the formation of the photoactivated $MIIG_t$ complex, as well as GTP-dependent disso-

Received for publication 15 January 1998 and in final form 22 May 1998.
Address reprint requests to Dr. Karim Fahmy, Institut für Biophysik und Strahlenbiologie der Albert-Ludwigs-Universität Freiburg, Albertstrasse 23, 79104 Freiburg, Germany. Tel.: 0761-203-5380; Fax: 0761-203-5016; E-mail: fahmy@ruf.uni-freiburg.de.

0006-3495/98/09/1306/13 $2.00

ciation of the complex can be monitored by ATR-FTIR difference spectroscopy. The experiments were particularly designed to characterize the infrared spectral changes that accompany light-induced formation of the functional $MIIG_t$ complex. A peptide comprising the 11 C-terminal residues of $G_{t\alpha}$ is shown to mimic the absorption changes evoked by heterotrimeric G_t, emphasizing the importance of the $G_{t\alpha}$ C-terminus in the interaction with MII. The potential of peptide synthesis as an alternative to site-directed mutagenesis for the conclusion of specific band assignments is demonstrated.

MATERIALS AND METHODS

Preparation of washed membranes and transducin

Bovine retinas were prepared from fresh cow eyes in dim red light and stored at −70°C. Rod outer segments (ROSs) were prepared from 100 frozen retinas as described (Papermaster, 1982), with minor modifications. Washed membranes were obtained from osmotically shocked ROSs, which were washed repeatedly in low ionic strength buffer. G_t was purified from illuminated ROSs by successive washes and hexyl agarose chromatography (Fung et al., 1981). G_t was eluted in buffer H (10 mM sodium phosphate, pH 6.0–7.6, 2 mM $MgCl_2$, 1 mM dithiothreitol, 0.1 mM phenylmethylsulfonyl fluoride) supplemented with 300 mM NaCl and the collected peak (~3 ml, typically 10–20 μM G_t) diluted with buffer H to a final concentration of 200 mM NaCl. For experiments in D_2O, the eluate was rebound to 1–2 ml of the column material. Buffer H in D_2O was prepared by evaporation of a previously buffered sodium phosphate solution and resuspension in D_2O. NaCl was added as powder; dithiothreitol and $MgCl_2$ were added from 500 mM and 1 M stock solutions in H_2O, respectively. The resin was washed three times with 10 ml of buffer H (D_2O) and stored on ice overnight. Transducin was eluted with 3 ml of buffer H (D_2O, 300 mM NaCl), and the eluate was diluted to 200 mM NaCl with buffer H (D_2O).

Reconstitution of rhodopsin into lipid vesicles

Washed membranes were solubilized in 1% *n*-octyl-β-D-glucoside (Bachem) and rhodopsin purified on con A-Sepharose (Pharmacia Biotech) as described by König et al. (1989b). Phosphatidylcholine from fresh egg yolk (Fluka; reporting approximate percentages of 33% 16:0, 14% 18:0, 30% 18:1, 14% 18:2, 4% 20:4 fatty acid chains) was lyophilized overnight and resuspended in 1 mM sodium phosphate buffer (pH 6.5). After sonication (5 min), the suspension was mixed with con A-purified rhodopsin (molar ratio 100:1). Samples were kept on ice for 1 h and then dialyzed for 24 h (8°C) against 4 liters of the same buffer in a flow cell with a 20,000 MW cutoff membrane. The dialyzed material was pelleted at 80,000 × *g* (4°C, 16 h). The pellets were directly resuspended in 200 μl buffer and frozen at −70°C. The reconstituted vesicles formed less MII than washed membranes but more MII than has been reported for suspensions of more rigorously (5 days, 10 liters) dialyzed phosphatidylcholine vesicles (Gibson and Brown, 1993). The more efficient MII formation can be attributed to the presence of residual detergent. Because MII formation in phosphatidylcholine vesicles was desired in this study, no attempts were made to remove residual detergent by washes of the collected pellets; nor were excessive dialysis times applied. Thus prepared vesicles produced ~70% MII at 17°C in buffer H, pH 6.8.

Fluorescence spectroscopy

A home-built fluorescence detection system with fiber optics in a 90° geometry for excitation and emission was employed to assay rhodopsin-catalyzed uptake of GTPγS by $G_{t\alpha}$ (Phillips and Cerione, 1988; Guy et al., 1990). Excitation was achieved with near-UV light of wavelengths between 290 and 310 nm, and emission was detected at wavelengths above 340 nm. Freshly eluted G_t solution (200 ml) was assayed for activity in 1.5 ml buffer H in the presence of photoactivated washed membranes in suspension before FTIR experiments.

FTIR spectroscopy

A home-built, temperature-controlled (17°C) attenuated total reflectance (ATR) unit with a horizontal trapezoidal internal reflection element (IRE), made from ZnSe (6 × 6 × 85 mm), was used to record difference spectra of washed membranes (1.5–2 nmol) in contact with aqueous solution. The membranes, taken from the same preparation as those used for the fluorescence assay, were slowly dried overnight on 3 cm^2 of the ZnSe surface under nitrogen gas. Buffer H (containing 200 mM NaCl) was added to the film, and the sample was allowed to equilibrate in the spectrophotometer for 1 h (after equilibration, the absorption of the sample was dominated by water absorption of 0.7 at 1640 cm^{-1}). For experiments in D_2O, membranes were allowed to equilibrate in buffer H (D_2O) for 8 h (after equilibration, the absorption maximum of membranes was 0.3–0.4 at 1657 cm^{-1}). Buffer was replaced during the measurements by perfusion with a G_t-containing solution through tubes connected to the sample compartment (1.5 ml). Interferograms were continuously measured and spectra were obtained by ratioing single beam spectra that corresponded to time intervals during which specifically induced changes took place. For rhodopsin activation, the sample was illuminated for 30 s through fiber optics using a slide projector (150 W) equipped with a yellow glass filter (GG 495; Schott). After illumination, 1 ml of 1 mM GTP in buffer H (200 mM NaCl) was added to a second compartment of the ATR cell, which was separated from the sample volume by a dialysis membrane (10,000 MW cutoff) 3 mm above the IRE surface. The nucleotide entered the sample volume slowly across the dialysis membrane and reached the IRE surface only by diffusion. In this way, mechanical perturbations at the IRE surface and concentration changes of other solutes (especially G_t) were prevented at the expense of a slower addition of GTP. Measurements in the presence of $G_{t\alpha}$-derived peptides were carried out by drying washed membranes in the presence of peptide (peptide:rhodopsin 100:1) onto the ATR crystal. Buffer was then added to the film to yield a final concentration of 2–3 mM peptide. $G_{t\alpha}$-derived peptides peptide 1 (aa 340–350), peptide 2 (aa 8–23), peptide 3 (aa 340–350, E342Q, D346N), and peptide 4 (peptide 3 with carboxy terminus amidated) were a generous gift of Prof. T. P. Sakmar. All measurements were carried out with a Bruker IFS 28 instrument with a spectral resolution of 2 cm^{-1}. Baselines were not corrected and spectra were not smoothed. To verify a physiological interaction between rhodopsin and G_t in ATR-FTIR samples, washed membranes were dried onto the upper part (covering 3 cm^2) of the inner wall of a fluorescence cuvette under nitrogen gas overnight, thereby simulating an ATR-FTIR sample on the IRE. The cuvette was filled with 1.5 ml of a solution of G_t (8 μM) in buffer H (200 mM NaCl), stirred gently on the bottom of the cuvette, and illuminated as above. The fluorescence increase observed after the addition of the nonhydrolyzable GTP analog GTPγS (final concentration 5 μM) proved that previously dried washed membranes maintain their catalytic activity for nucleotide exchange in G_t.

RESULTS AND DISCUSSION

Interaction of G_t with disk membranes

The measurement of infrared asborption changes of the rhodopsin to MII transition in washed membranes in the presence of G_t is based on the observations by Kühn (1980) and Liebman and Sitaramayya (1984), who showed that G_t can bind to disk membranes in the dark. The nature of the binding site is controversial and may either be provided by

membrane lipids (Matsuda et al., 1994) or reside in unbleached rhodopsin itself (Salamon et al., 1996). Here this membrane association is followed with infrared spectroscopy by recording absorption spectra of washed membranes attached to an IRE perfused with a buffer solution containing freshly prepared G_t. Before perfusion, a stable absorption baseline is recorded (Fig. 1 *a*), indicating equilibration of the rhodopsin film with the buffer. Only the association of G_t with the membranes increases the G_t concentration near the IRE surface to a level high enough for infrared detection. Free G_t in the buffer is not observed spectroscopically, because of the small penetration depth of the infrared beam (Harrick, 1983) and the submillimolar concentration of G_t in the buffer. Fig. 1 *b* shows the increase of amide I and amide II absorption bands at 1638 cm^{-1} and 1555 cm^{-1}, respectively, as a consequence of G_t associating with the rhodopsin film in the dark (see below). The amide I and II frequencies show that the absorption increase is not due to rhodopsin, because the amide I and II bands of rhodopsin are located at 1657 cm^{-1} and 1546 cm^{-1}, respectively. The lower amide I frequency of G_t agrees with the existence of β-strands in $G_{t\alpha}$ (Noel et al., 1993) and, particularly, $G_{t\beta\gamma}$ (Sondek et al., 1996), which are expected to absorb below 1640 cm^{-1} (Krimm and Bandekar, 1986; Hadden et al., 1995). The magnitude of the amide absorption increases reflects a lower limit for the membrane association because baseline perturbations prevent spectral recordings during the first 3 min after the addition of G_t. An accurate calibration of the infrared absorption with respect to the concentration of G_t is hampered by the fact that the absorption increase is not strictly proportional to the amount of bound G_t. This is due to the decrease in the evanescent field of the IR-beam with increasing distance from the IRE. Therefore, G_t bound to the top layer of the adsorbed washed membranes contributes less to the entire absorption than G_t that has penetrated more deeply into the membrane stacks. Complete saturation of washed membranes with G_t in these experiments, however, can be ruled out, because an increase in the G_t concentration could still evoke an increase of infrared absorption (data not shown).

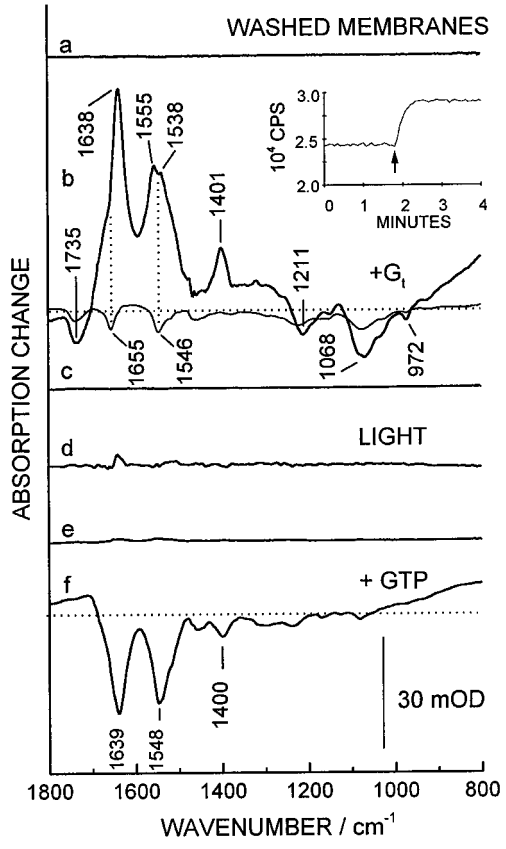

FIGURE 1 Consecutively recorded difference spectra from washed membranes attached to a ZnSe IRE in contact with buffer H (200 mM NaCl), pH 7.2. (*a*) Baseline before perfusion of the buffer compartment (256 scans). (*b*) Absorption changes evolving in the dark (starting 3 min after the addition of G_t) over 30 min of perfusion with G_t (10 μM) in the same buffer (1024 scans). The thin line represents absorption changes during a 2-min interval starting 3 min after the addition of G_t. (*c*) Baseline after saturation of washed membranes with G_t in the dark (128 scans). (*d*) Light-induced absorption changes of G_t-saturated washed membranes after 30 s of illumination (128 scans). (*e*) Absorption changes developing 3 min after the end of illumination and recording of trace d (128 scans). (*f*) Absorption changes developing over 30 min after the addition of GTP (0.5 mM final concentration) to the buffer (1024 scans). Horizontal dotted lines correspond to zero absorption change. Measurements were carried out at pH 7.2, 17°C. (*Inset*) Intrinsic fluorescence (expressed in counts per second recorded by photomutiplier) of $G_{t\alpha}$ as a function of time. A simulated FTIR sample (see Materials and Methods) in contact with a solution of freshly prepared G_t (in buffer H, 200 mM NaCl) was photoactivated, and the fluorescence of G_t continuously recorded. The arrow indicates the addition of 50 μl of a GTPγS solution in the same buffer (final concentration 5 μM).

An interpretation of absorption changes in Fig. 1 *b* as pure G_t bands would not be correct. The net increase in G_t absorption is superimposed on a loss of absorption by rhodopsin. This is obvious from absorption changes measured over 2 min at an early state of dark association, i.e., 3–5 min after the addition of G_t (Fig. 1 *b*, *thin line*). During this time, the decrease in rhodopsin absorption at 1657 cm^{-1} and 1547 cm^{-1} is not offset by the increase in amide I and II bands of G_t. In particular, the decrease in the 1735 cm^{-1} band, characteristic of the lipid ester carbonyl stretching modes in photoreceptor membranes (DeGrip et al., 1985), appears concomitantly with the reduction of absorption by rhodopsin and argues for a physical perturbation of the membranes during G_t association. Additional absorption changes are observed between 1000 and 1300 cm^{-1} and are indicative of altered P-O stretching modes. An absorption increase is expected in this range because G_t carries GDP in the binding pocket as a result of GTP hydrolysis during protein preparation. However, the observed bands are negative and their magnitude relative to the amide absorption is too large to be caused by a single nucleotide in the heterotrimer. These observations can be explained by swelling of the membranes upon the addition of G_t. This causes a dilution of membrane fragments within the effective penetration depth of the infrared beam and thus reduces absorption from lipid esters and phosphates as well as amide I and II bands of rhodopsin. Concomitantly, the absorption of G_t

increases. This indicates that, via penetration into the membrane stacks, transducin becomes enriched at the IRE surface at the expense of absorption of washed membranes. The absorption increase observed at 1400 cm^{-1} is probably caused by the symmetrical COO^- stretching mode of unprotonated carboxylic acid groups present on G_t, as expected at pH 7.2. The absorption changes attributable to dark binding of G_t were completed after 30–60 min. After this time, a flat baseline was again recorded (Fig. 1 *c*).

Subsequent illumination of the G_t-saturated membranes for 30 s causes small absorption changes, shown for comparison of the band magnitudes in the same scale in Fig. 1 *d*. These difference bands reflect the transition from G_t-loaded membranes in the dark to the light-activated $MIIG_t$ complex. Because the membranes were already efficiently loaded with G_t in the dark, almost no further net uptake of free G_t from the buffer occurs on the time scale of illumination and spectral recording of trace d. In addition, diffusion of free G_t into and out of the membranes takes much longer than the time needed for formation of the complex between dark-bound G_t and MII (Schleicher and Hofmann, 1987). Therefore, the light-induced absorption changes can be recorded without interference with absorption changes from repartitioning of G_t into the washed membranes. During the 3 min after the recording of trace d in Fig. 1, only very small absorption increases are observed at 1640 cm^{-1} and 1550 cm^{-1} (Fig. 1 *e*).

To verify that a functional complex between photoactivated rhodopsin and transducin was formed upon illumination, GTP was added to the buffer. Fig. 1 *f* shows the ensuing decrease in amide I and II absorption expected during dissociation of transducin from the membranes and thus from the IRE surface. In contrast to the initial membrane association, the absorption changes at 1735 cm^{-1} and between 1000 and 1300 cm^{-1} are barely visible. This indicates that swelling of the membranes during G_t association (Fig. 1 *b*) is essentially irreversible. Thus the amide I and II modes in Fig. 1 *f* probably better reflect a pure transducin infrared spectrum than those in Fig. 1 *b*. The lack of structure in the amide absorption bands in trace f versus b can easily be explained by the lack of membrane shrinking in trace f versus membrane swelling in trace b. This is supported by the exact coincidence of the shoulder at 1657 cm^{-1} and the dip at 1546 cm^{-1} in the amide I and II bands, respectively (Fig. 1 *b*), with the negative peak absorptions of rhodopsin in the swelling membranes (Fig. 1 *b*, *thin line*). Because of the involvement of membrane lipids and phosphates as well as contributions from MII decay after GTP addition, a detailed interpretation in terms of distinct conformational changes in G_t cannot be based on comparison of Fig. 1 *b* with Fig. 1 *f*. Likewise, the nature of the binding site of G_t (lipids or rhodopsin) cannot be deduced from the infrared absorption changes. However, the detection of absorption decreases at 1639 cm^{-1} and 1548 cm^{-1}, i.e., at positions different from the vibrations in rhodopsin, indicates that GTP specifically releases G_t from washed membranes rather than causing a detachment of the membrane stacks themselves from the IRE surface. The absorption decreases can also not be explained by merely washing G_t off the IRE surface, because the nucleotide was added slowly by dialysis (see Materials and Methods), thus avoiding mechanical perturbations and concentration changes encountered with flow injection methods. Therefore, G_t dissociation occurred in the presence of a constant G_t concentration in the bulk water phase, which allows one to attribute G_t dissociation from the IRE to the specific action of the nucleotide on the $MIIG_t$ complex. This argues for the biological integrity of the protein-protein interactions under the conditions of the experiment. Because the transducin pool in the buffer (~10 nmol) was large as compared to the amount of dark-bound G protein, G_t (in the GDP-bound form) in the bulk could reoccupy binding sites that have been liberated upon GTP-induced complex dissociation. Consequently, the net loss of G_t from the IRE occurred slowly and had not been completed when trace f was recorded. This explains why the magnitude of the dissociation signal is smaller than that of dark association (Fig. 1 *b*). Further evidence for a physiological interaction of rhodopsin and G_t is presented in the inset. A simulated ATR-FTIR sample catalyzes nucleotide exchange in G_t, as measured by the fluorescence increase of the $G_{t\alpha}$ subunit upon binding the nonhydrolyzable GTP analog GTPγS (see Materials and Methods). Here a concentration jump was applied. Accordingly, the reaction could proceed much faster, demonstrating efficient receptor-G protein coupling in the simulated ATR-FTIR sample.

In summary, the results presented in Fig. 1 show that an entire cycle of nucleotide-dependent receptor G protein interaction can be recorded under the conditions of the ATR-FTIR experiment and in the presence of bulk water.

Spectral features of the $MIIG_t$ complex

The focus of the present study is to characterize the formation of the photoactivated $MIIG_t$ complex on the basis of infrared absorption changes shown in Fig. 1 *d*. This difference spectrum is replotted with ordinate expansion in Fig. 2 *a*. It clearly differs from the absorption changes obtained in the absence of G_t under otherwise identical conditions (Fig. 2 *b*). The difference bands are in general agreement with previously published spectra of MII formation in hydrated films (Ganter et al., 1989; Klinger and Braiman, 1992; Maeda et al., 1993). Deviations can be explained by the different contribution of anisotropically arranged infrared transition moments when probed in the ATR geometry, as well as by the presence of bulk water in the ATR cell. For example, the negative band at 1654 cm^{-1} is much more pronounced when measured with the ATR technique, resembling the absorption in hydrated films when anisotropy is abolished by detergent solubilization (Fahmy et al., 1993). The intense MII marker band at 1644 cm^{-1} in hydrated films (Klinger and Braiman, 1992) shifts down by 2–3 cm^{-1} when observed by the ATR technique.

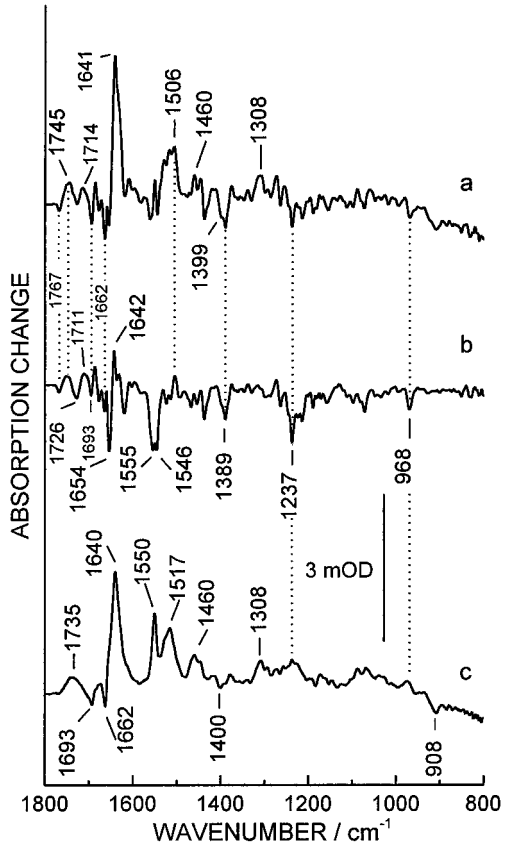

FIGURE 2 Light-induced absorption changes of washed membranes in H_2O. Conditions as in Fig. 1. (*a*) MII formation in the presence of G_t (same spectrum as in Fig. 1 *d*). (*b*) MII formation in the absence of G_t measured under identical conditions. This spectrum has been scaled to the size that corresponds to compensation of the 1767 cm^{-1} band after subtraction from trace a. (*c*) Trace a minus trace b, representing the effects of G_t on the difference spectrum of MII formation; trace c is shown in the same scale as trace a.

G_t-induced infrared absorption changes at pH 7.2 (Fig. 2 *c*) are obtained by subtracting trace b from trace a to minimize the negative C═O stretching band of protonated Asp^{83} at 1767 cm^{-1}. This group is not involved in G_t activation (Fahmy et al., 1993). Because it is located in the hydrophobic core of the protein, it is also unlikely to undergo binding interactions with G_t. Therefore, normalization to the 1767 cm^{-1} band provides a reasonable criterion for avoiding subtraction artifacts in the determination of G_t-dependent absorption changes. This is further supported by the fact that the subtraction does not cause appreciable residual intensity of the strong vibrational band of 11-*cis* retinal at 1237 cm^{-1}. Correspondingly, the same amount of photoreacted rhodopsin is subtracted within the accuracy of the baseline. Normalization to the Asp^{83} band of unbleached rhodopsin, rather than to the 1237 cm^{-1} band itself, prevents subtraction artifacts, particularly in the 1700–1800 cm^{-1} range. This allows a reliable investigation of G_t-induced changes in this spectral range (see below), whereas bands between 1100 and 1300 cm^{-1} are little affected by G_t. The predominant absorption changes during $MIIG_t$ complex formation occur in the amide I region (1620–1690 cm^{-1}) and the amide II region (1520 to 1560 cm^{-1}). The major effect of G_t is the increase in a 1662 cm^{-1} (negative)/1640 cm^{-1} (positive) difference band. Absorption changes at these peaks are already present in the difference spectrum of MII formation in the absence of G_t. Likewise, an absorption band at 1693 cm^{-1}, which is also found in unbleached rhodopsin, does not cancel after spectral subtraction. In the amide II range, G_t induces a positive band at 1550 cm^{-1} that is not observed in rhodopsin/MII difference spectra. Similarly, positive bands that are observed neither in rhodopsin nor in MII occur below the typical amide II spectral range at 1517 cm^{-1} and at 1460 cm^{-1}. Less prominent but reproducibly observed bands can be discerned at 1308 cm^{-1} (positive) and 908 cm^{-1} (negative).

Deviations from the normal MII difference spectrum are also observed in the spectral range of C═O stretching vibrations between 1700 cm^{-1} and 1800 cm^{-1}. The pattern of absorption bands of protonated carboxylic acid residues (DeGrip et al., 1985) has been assigned to amino acids Asp^{83}, Glu^{113}, and Glu^{122} in the transmembrane part of rhodopsin (Jäger et al., 1994; Fahmy et al., 1993; Rath et al., 1993). These bands are reproduced in the presence of G_t (Fig. 2 *a*). However, the usual features are superimposed on a broad positive band centered at 1735 cm^{-1}, which becomes clearly and reproducibly visible after subtraction of the control spectrum. Upon binding of G_t to washed membranes in the dark, an absorption decrease is observed at this frequency (Fig. 1 *b*). In contrast to the slow binding process, however, the light-induced absorption changes presented in Fig. 2 were recorded within 1 min after 30 s of illumination and thus are unlikely to be affected by slow binding or dissociation processes. Even after the end of illumination, only very small additional binding of G_t to the membranes is observed (Fig. 1 *e*). Finally, the sign of the 1735 cm^{-1} band in Fig. 2 *c* is opposite the absorption change related to lipid ester carbonyl vibrations during association of G_t with membranes (Fig. 1 *b*). Thus at least part of the broad band may be caused by the C═O stretching vibration of a carboxylic acid group that becomes protonated in the $MIIG_t$ complex. A stably protonated carboxylic acid group would cause a negative and a positive lobe instead of the purely positive band at 1735 cm^{-1}. The occurrence of an additional negative absorption at 1400 cm^{-1}, typical of the symmetrical COO^- stretch of a carboxylate, agrees with the inferred light-induced protonation. This mode causes the shoulder on the negative band at 1389 cm^{-1} (Fig. 2 *a*), which is visible as a negative band at 1400 cm^{-1} after spectral subtraction in Fig. 2 *c*.

Influence of extra MII formation and pH

The reference spectrum in Fig. 2 *b* has been recorded in the buffer used for the G_t-containing sample. This eliminates possible pH-dependent spectral alterations that may otherwise be confused with G_t-dependent bands after spectral

subtraction. However, MI and MII coexist in a pH-, temperature-, and ionic strength-dependent manner (Parkes and Liebman, 1984; Gibson and Brown, 1993; DeLange et al., 1997). Because G_t shifts this equilibrium to MII (extra MII effect; Emeis and Hofmann, 1981), the subtraction procedure may also generate absorption differences that are related to different amounts of MI and MII. It is important to analyze how this may qualitatively and quantitatively affect the features ascribed to the $MIIG_t$ complex. For this purpose, the pH 7.2 reference spectrum (Fig. 2 *b*) has been subtracted from a pure MII difference spectrum recorded at pH 5.5, resulting in the MII minus MI absorption differences shown in Fig. 3 *f*. These absorption changes reflect the maximum contribution of extra MII formation to the trace in Fig. 2 *c*. The MII minus MI changes exhibit the characteristic bands of Asp^{83} and Glu^{122}, which cause negative and positive bands in the 1700–1800 cm^{-1} range. This is in stark contrast to the broad and structureless absorption increase caused by G_t around 1735 cm^{-1} (Fig. 2 *c*). Therefore, this feature cannot be explained by extra MII formation. Although the MII/MI-related changes do not contribute significant integral intensity to the 1700–1800 cm^{-1} range, they may have an influence on band shapes. This can be appreciated in Fig. 3 *c*, where G_t-induced bands at pH 7.2 have been obtained by subtracting the pure MII difference spectrum (pH 5.5) from the difference spectrum of the complex (Fig. 2 *a*). The flanks of the 1735 cm^{-1} band have become more concave as compared to their convex appearance in Fig. 2 *c*. As expected, the alternative subtraction neither abolishes nor enhances the G_t-dependent absorption increase, demonstrating that this feature is clearly related to the interaction of MII and G_t and not to a shift in the photoproduct equilibrium. Likewise, the G_t-induced modes at 1550, 1517, 1131, and 908 cm^{-1} (Figs. 2 *c* and 3 *c*) cannot be explained by the enrichment of the MII state at the expense of MI, because no corresponding bands are found at these positions in Fig. 3 *f*. Only the bands at 1692, 1640, and 1460 cm^{-1} agree in frequency and relative intensity with G_t-dependent vibrational changes. The 1663 cm^{-1} absorption decrease in MII versus MI corresponds to a less pronounced negative band at this frequency in Fig. 3 *c*. Finally, the MI-to-MII transition is accompanied by small chromophore absorption changes of hydrogen out-of-plane modes between 950 and 980 cm^{-1} (Maeda et al., 1993; Ohkita et al., 1995). The lack of residual bands at these frequencies in Fig. 3 *c* is again inconsistent with extra MII formation being responsible for even those bands that resemble MI/MII differences. It is not surprising that extra MII formation is not the predominant process responsible for G_t-dependent spectral changes, because the experimental conditions do not strongly favor the MI state in the absence of G_t, as is required for extra MII formation. The latter is typically observed at 4°C and pH 8 (König et al., 1989a), corresponding to ~10% MII in the absence of G_t. In contrast, 68% MII are formed under the conditions of the FTIR experiment. This can be calculated by simulating the trace in Fig. 2 *b* by a weighted sum of MI and MII ATR-FTIR difference spectra recorded at pH 8.8 (5°C) and 5.5 (17°C), respectively, and agrees with previous results on washed membranes (Parkes and Liebman, 1984; DeLange et al., 1997). Therefore, only ~30% of the pigment is in the MI form and thus can undergo extra MII formation. In addition, not all rhodopsin molecules may be accessible to G_t in the membrane stacks used here, as compared to the suspensions employed for extra MII detection. Nevertheless, some extra MII formation under the conditions of the FTIR experiment can be inferred from inspection of chromophore vibrational modes. At pH 7.2, the band of 11-*cis* retinal at 968 cm^{-1} does not appear to be perfectly compensated (Fig. 2 *c*) after subtraction of a difference spectrum recorded at the same pH. The similarity of the residual difference band with that of the MII minus MI difference spectrum at 968/950 cm^{-1} (Fig. 3 *f*) indicates that MII/MI related absorption changes contribute to the trace in Fig. 2 *c*, whereas they are compensated in Fig. 3 *c*. However, none of the G_t-induced bands labeled in Fig. 2 *c* are missing, and peak frequencies are not affected by the alternative subtraction method. This indicates that near pH 7, at 17°C and 200

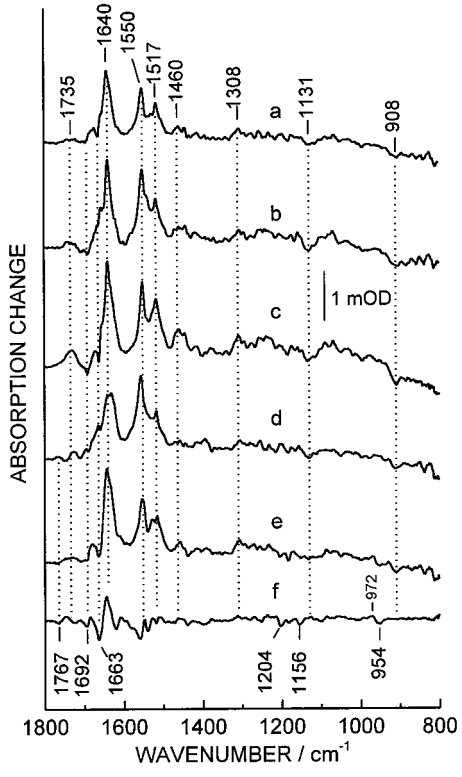

FIGURE 3 Influence of pH on G_t-induced bands. A pure MII difference spectrum (obtained at pH 5.5) was subtracted from difference spectra recorded in the presence of G_t in buffer H at pH 6 (*a*), at pH 6.8 (*b*), at pH 7.2 (*c*), and at pH 7.6 (*d*). (*e*) Trace d plus 1.4 * trace f. This corresponds to subtraction of a reference spectrum containing 43% MI (pH 8.8, 5°C) and 57% MII (pH 5.5, 17°C) absorption changes from the pH 7.6 differences measured in the presence of G_t. (*f*) Maximum (32%) extra MII effect at pH 7.2, calculated by subtracting the pH 7.2 difference spectrum (containing 68% MII, Fig. 2 *b*) from a difference spectrum obtained at pH 5.5 (100% MII). All traces are shown in a common scale indicated by the scale bar. Conditions are as in Fig. 1.

mM NaCl, the absorption changes attributable to MII-G_t interaction clearly dominate the more subtle spectral features ascribable to extra MII formation.

In addition to the influence of pH on the reference spectrum, and thus on the appearance of G_t-induced absorption bands, pH affects the infrared-spectroscopic properties of the $MIIG_t$ complex itself. G_t-dependent absorption changes have been determined from spectra measured in the presence of G_t between pH 6.0 and 7.6 (Fig. 3, *a–d*), by subtracting the pure MII difference spectrum. Obviously, G_t-dependent changes are resolved between pH 6 and pH 7.6 (Fig. 3, *a–c* and *e*). The amide I and II absorption increases and the positive bands at 1517 cm^{-1} and 1460 cm^{-1} are essentially pH independent. In contrast, a clear pH dependence is observed for the 1735 cm^{-1} vibration, which is present at pH 7.2 but markedly reduced at pH 6 and 7.6, thereby correlating roughly with the pH rate profile of transducin activation (Cohen et al., 1992; Fahmy and Sakmar, 1993). At pH 7.6, however, MI absorption in the presence of G_t becomes too large to allow an accurate generation of G_t-induced bands by subtraction of a pure MII difference spectrum. Therefore, the 1767 cm^{-1} band cannot be compensated with a subtraction factor that avoids unrealistically large residual bands in the fingerprint spectral range (Fig. 3 *d*). In agreement with this explanation, a broad but weak 1735 cm^{-1} band reappears (Fig. 3 *e*) when the MII minus MI differences (Fig. 3 *f*) are added to trace d with a weight that corresponds to the subtraction of MII and MI differences in a percentage ratio of 57:43.

In summary, extra MII formation in the presence of G_t cannot account for the G_t-induced absorption changes either qualitatively or quantitatively. Therefore, the described bands must be assigned to specific interactions in the $MIIG_t$ complex. G_t-induced bands have been reported in an earlier study using transmissive FTIR difference spectroscopy (Nishimura et al., 1996). Clear correspondence, however, is seen only for the 1640 cm^{-1} absorption increase. The reported vibrational changes in the amide II and III spectral range are not confirmed here, except for the agreement in the 1308 cm^{-1} band. The small 1400 cm^{-1} absorption decrease has also been observed with transmissive FTIR difference spectroscopy, but the 1735 cm^{-1} band was not detected. Its pronounced pH sensitivity suggests that it is caused by the C═O stretching vibration of a titratable carboxylic acid group which, near pH 7, becomes protonated in the $MIIG_t$ complex. Discrepancies with respect to the transmissive measurements are probably due to the very different experimental conditions. With the ATR technique, formation of the photoactivated complex is accomplished in 30 s at 17°C, whereas the transmissive method was applied at −8°C under conditions that favor MI and slow down complex formation to the order of 30–60 min. At the lower temperature, conformational changes of the complex as well as membrane fluidity may become restricted. Furthermore, the double subtraction and baseline correction procedures needed to correct for MI, uncomplexed MII, and time-dependent changes in the transmissive spectra reduce the signal-to-noise ratio and may cause some ambiguity concerning the sign of certain bands. These problems have been circumvented in the present study. The choice of a pH near 7 allows optimal binding of G_t to rhodopsin. Predominant MII formation in the absence of G_t is achieved, because of an elevated temperature at which a severe reduction of the fluidity of the washed membranes can be excluded (Chabre, 1975; Coke et al., 1986). The G_t-induced bands thus obtained are about three times larger than in transmissive spectroscopy and, therefore, are less affected by interference with extra MII formation as compared to low-temperature experiments.

The $MIIG_t$ complex in phosphatidylcholine vesicles

Association of G proteins with membranes is mediated by lipid modifications (Kokame et al., 1992; for a review see Casey, 1994). To assess whether specific lipids of the washed membranes also play a critical role in the shift of infrared-active modes during MII-G_t interaction, G_t-induced absorption changes were recorded with purified rhodopsin reconstituted into phosphatidylcholine vesicles. Association of G_t with phosphatidylcholine vesicles in the dark and GTP-dependent dissociation were accompanied by spectral changes almost identical to those of the native system (data not shown). Light-induced differences at pH 6.8 are plotted in Fig. 4. At this pH, a MII:MI photoproduct mixture is obtained which nearly matches that in washed membranes at pH 7.2. This agrees with the lower pK of the MI-MII equilibrium in phosphatidylcholine vesicles versus washed membranes (Gibson and Brown, 1993). Here, however, MII formation is additionally facilitated by avoiding excessive removal of detergent during reconstitution (see Materials and Methods). FTIR difference spectra of MII formation in minimally unsaturated phosphatidylcholine vesicles have also been described previously (DeGrip et al., 1985). The prominent G_t-dependent absorption increase is again at 1640 cm^{-1}, and the distortion of the carbonyl stretching bands between 1700 and 1800 cm^{-1} is already discernible (Fig. 4 *a*) without subtraction of the absorption changes of uncomplexed rhodopsin. After subtraction of the reference spectrum recorded under identical conditions in the absence of G_t (Fig. 4 *b*), G_t-induced bands described for washed membranes are very well reproduced, including the appearance of small bands at 1308, 1400, and 1460 cm^{-1}, and the absorption decreases at 908 and 1693 cm^{-1} (Fig. 4 *c*, *dotted line*). The absorption decrease at 1662 cm^{-1} is more pronounced in phosphatidylcholine vesicles, and a small additional negative structure at 1709 cm^{-1} occurs. However, residual chromophore absorption bands at 1237 cm^{-1} and 968 cm^{-1} (Fig. 4 *c*, *dotted line*) indicate that compensation of the 1767 cm^{-1} band is only achieved by subtracting the pH 6.8 reference spectrum to a larger extent than would be necessary to match identical amounts of photoreacted rhodopsin. This can be explained by extra MII formation, i.e.,

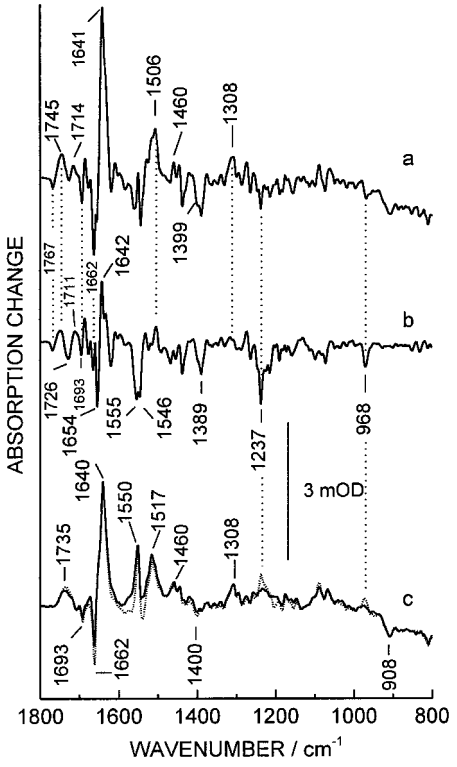

FIGURE 4 Influence of G_t on difference spectra in reconstituted phosphatidylcholine vesicles at pH 6.8 (other conditions as in Fig. 1). (*a*) Absorption changes in the presence of G_t. (*b*) Absorption changes in the absence of G_t, scaled to the size of the 1767 cm^{-1} band in trace *a*. (*c*) Solid trace: G_t-induced absorption changes obtained by subtracting a pure MII difference spectrum from trace a; dotted trace: G_t-induced absorption changes obtained by subtracting trace b from trace a.

a smaller MII content in the reference spectrum, which thus exhibits a smaller 1767 cm^{-1} band than the difference spectrum of the complex. Correspondingly, the reference spectrum has to be scaled up to match the Asp^{83} absorption. The fingerprint modes become scaled up as well and, therefore, become "oversubtracted." This results in positive residual bands that in the original difference spectra have negative signs. In agreement with this explanation, subtraction of a pure MII difference spectrum better compensates the chromophore absorption changes at 1237 and 968 cm^{-1} (Fig. 4 *c*, *solid line*). Although the effect of extra MII formation is slightly larger than in washed membranes, the alternative subtraction method again neither creates nor abolishes any of the G_t-induced bands, showing that also in phosphatidylcholine vesicles the spectral contribution of extra MII formation is small as compared to the G_t-induced effects. In particular, the 1700–1800 cm^{-1} spectral range itself is only little affected by the choice of the reference spectrum. Thus, taking extra MII formation into account, compensation of the 1767 cm^{-1} band leads again to a reasonable correction for different amounts of photoactivated samples in the two independent experiments. Because the broad 1735 cm^{-1} band is well reproduced in phosphatidylcholine vesicles, it cannot be explained by protonation of carboxylic acid groups of phosphatidylserine lipids during MII-G_t interaction in washed membranes.

In summary, the close correspondence of the G_t-induced bands in phosphatidylcholine vesicles to those in washed membranes shows that net charge and nature of lipid side chains have only very little influence on structural changes accompanying $MIIG_t$ complex formation.

Mimicking the $MIIG_t$ complex by peptide binding

The magnitude of G_t-induced absorption changes is comparable to that of the difference bands occurring during rhodopsin photoactivation alone. This indicates that only a small part of the G_t structure is involved in the interactions monitored by FTIR spectroscopy. It has been shown that a peptide, comprising the C-terminal amino acids 340–350 of $G_{t\alpha}$, stabilizes MII and thus mimics the effect of G_t (Hamm et al., 1988). This peptide (peptide 1: IKENLKDCGLF) was tested here for its ability to evoke infrared absorption changes in washed membranes similar to G_t. Peptide-induced alterations are much less pronounced in the light-induced absorption changes (Fig. 5 *a*) than those evoked by G_t. However, after spectral subtraction of a difference spectrum recorded in the absence of peptide (Fig. 5 *b*), bands are resolved (Fig. 5 *c*) that resemble those caused by G_t (Fig. 5 *e*). The broad feature at 1735 cm^{-1} is reproduced, as is the 1550 cm^{-1} absorption increase. The 1517 cm^{-1} band is present, but its intensity is reduced. Instead of a 1662/1640 cm^{-1} difference band, the peptide causes a 1662/1657 cm^{-1} absorption change, and only a shoulder is present at 1640 cm^{-1}. The smaller G_t-induced changes at 1400 cm^{-1} (negative), 1308 cm^{-1} (positive), and 908 cm^{-1} (negative) are not observed with peptide 1.

Taking into account that peptide 1 comprises only ~10% of the mass of the G_t trimer, it is surprising that it nevertheless induces some of the salient features described for the interaction of the holo protein with MII. In contrast, an N-terminal peptide (peptide 2: aa 8–23: EEKHSRELEKKLKEDA) that blocks rhodopsin G_t interaction but does not stabilize MII (Hamm et al., 1988) failed to reproduce G_t-induced infrared absorption changes (Fig. 5 *d*). Except for the negative band at 1662 cm^{-1}, the amide I and II changes are clearly different from G_t-and peptide 1-induced alterations. Furthermore, because the 1735 cm^{-1} absorption increase is not evoked by peptide 2, the band cannot be ascribed to a nonspecific action of peptides or proteins on washed membranes. These results strongly argue for a specific and native-like interaction of peptide 1 with MII and imply that the C-terminus of $G_{t\alpha}$ is largely responsible for the infrared absorption changes ascribed to $MIIG_t$ complex formation. The lack of the strong amide I absorption at 1640 cm^{-1} in Fig. 5 *c* may also be related to the lack of the nucleotide binding pocket. The latter is expected to undergo a conformational change, which is mediated by the $G_{t\alpha}$ C-terminus upon receptor binding (Onrust et al., 1997). Finally, the normal appearance of the broad 1735 cm^{-1}

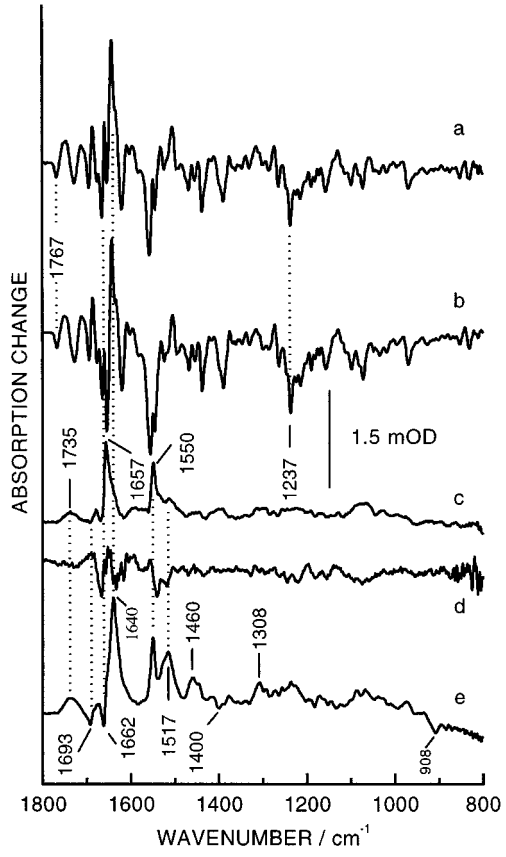

FIGURE 5 Influence of $G_{t\alpha}$-derived peptides on the difference spectrum at pH 6.8 in washed membranes (peptide concentration 2–3 mM; other conditions as in legend to Fig. 1). (*a*) Absorption changes in the presence of peptide 1 (amino acids 340–350). (*b*) Absorption changes in the absence of peptide, scaled to the size of the 1767 cm^{-1} band in trace a. (*c*) Peptide 1-induced absorption changes obtained by subtracting trace b from trace a. (*d*) Absorption changes induced by the $G_{t\alpha}$-N-terminal peptide 2 (amino acids 8–23), measured under the same conditions and calculated analogously as for peptide 1-induced changes. (*e*) G_t-induced absorption changes (same as in Fig. 2 *c*).

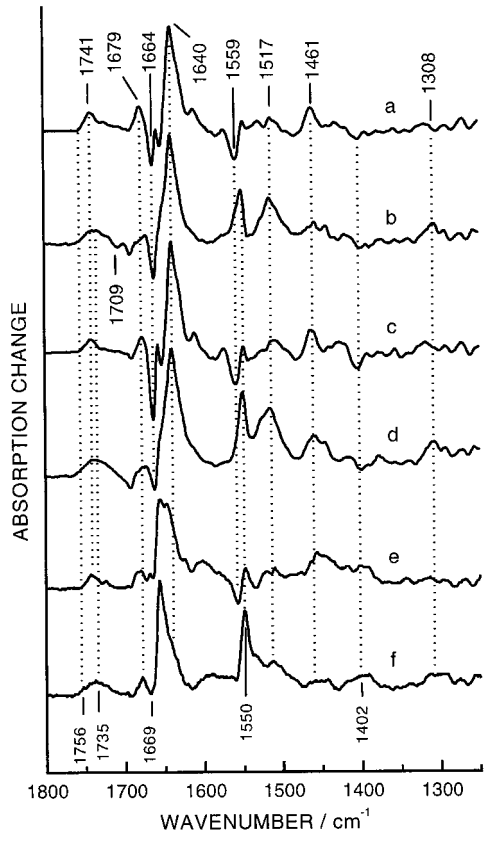

FIGURE 6 Influence of H/D exchange on G_t- and peptide-induced absorption changes during photoactivation. (*a* and *b*) G_t-induced absorption changes in phosphatidylcholine vesicles, measured in D_2O and H_2O (as in Fig. 4 *c*, *solid trace*), respectively. (*c* and *d*) G_t-induced absorption changes in washed membranes, measured in D_2O and H_2O (as in Fig. 2 *c*), respectively. (*e* and *f*) Peptide 1-induced absorption changes in washed membranes, measured in D_2O and H_2O (as Fig. 5 *c*), respectively.

vibration in Fig. 5 *c* excludes a contribution of carbonyl stretches from lipid modifications on G_t to the difference spectra.

Effect of H/D exchange on the carbonyl stretching frequency range

The nature of the G_t-induced absorption increase around 1735 cm^{-1} was further investigated by recording difference spectra of the $MIIG_t$ complex formation in the presence of D_2O. No isotope sensitivity is expected for a lipid carbonyl stretch, whereas C═O stretching vibrations of protonated carboxylic acid groups can be identified by their frequency downshift in D_2O. Fig. 6 compares the light-induced absorption changes in D_2O (Fig. 6 *a*) versus H_2O (Fig. 6 *b*) obtained with G_t in phosphatidylcholine vesicles, G_t in washed membranes (Fig. 6, *c* and *d*), and with peptide 1 in washed membranes (Fig. 6, *e* and *f*). In all cases, the broad 1735 cm^{-1} band in H_2O is replaced by a narrower band at 1741 cm^{-1} in D_2O, because of pronounced isotope sensitivity in the low-frequency part of the 1735 cm^{-1} band. A small downshift in the high-frequency part is also discernible, as shown by the band positions relative to the 1756 cm^{-1} line in Fig. 6. The isotope sensitivity suggests that in all three systems, protonation of a carboxylic acid group contributes to the broad 1735 cm^{-1} absorption increase. The position of the downshifted C═O stretch in D_2O is expected in the 1710–1720 cm^{-1} range, but it is difficult to discern in the native system (Fig. 6 *c*), where it may overlap with the flank of the broad absorption decrease toward 1700 cm^{-1}. In phosphatidylcholine vesicles in H_2O, a small additional negative dip is present at 1709 cm^{-1} (Fig. 6 *b*). In this case, the lack of the structure in D_2O (Fig. 6 *a*) would agree with the shift of intensity into this frequency range. Apparently, the D_2O-sensitive component causes a broad band at the expense of peak intensity. The isotope effect between 1700 and 1800 cm^{-1} in the three systems is best explained by a broad C═O stretching mode of a protonated carboxylic acid in $MIIG_t$ absorbing at ~1730 cm^{-1}, which overlaps with a narrower band at 1741 cm^{-1} (exhibiting little or no isotope sensitivity). Only the superposition of

both features causes the broad absorption increase at 1735 cm^{-1} in H_2O. The broadness of the isotope-sensitive low-frequency component may be explained by different models:

1. It may be caused by a population of carboxylic acid groups exhibiting different C═O stretching vibrations. These groups may become partly protonated as a consequence of a slight pH shift at the membrane surface after $MIIG_t$ complex formation.

2. A single C═O group may undergo different hydrogen bonding interactions in $MIIG_t$, giving rise to a range of stretching frequencies.

Regarding model 1, light-induced alteration of the mode of membrane association of the G_t trimer may be thought to affect net membrane charge and local proton concentration. However, it is not clear how a small peptide would do so. In addition, replacement of the native phosphatidylserine-containing lipids by phosphatidylcholine changes the electrostatic properties of the membrane and its interaction with G_t (Matsuda et al., 1994), but does not affect the formation of the 1735 cm^{-1} absorption. Therefore, it is more likely that protonation of a specific carboxylic acid group, as proposed in model 2, is responsible for this band. Its appearance would be compatible with a group near the water-exposed surface of rhodopsin or G_t, rather than a buried residue. Infrared absorption changes from surface residues of both proteins are actually expected, because the protein-protein or protein-peptide interactions will preferentially affect exposed residues. Furthermore, the complete canceling of the difference bands of Asp^{83}, Glu^{113}, and Glu^{122} in the G_t-induced spectra indicates that these internal residues are indeed not affected by complex formation.

It is difficult to explain the isotope sensitivity of the 1735 cm^{-1} absorption without the superposition of two independent bands. If a single C═O stretch is assumed for the entire feature, one may speculate that the broad band in H_2O is caused by coupling of the C═O stretching mode to OH bending modes of surrounding water molecules. Isotope exchange would remove this coupling, giving rise to a narrower band at 1741 cm^{-1} in D_2O. Without site-directed mutagenesis it will be difficult to decide between the suggested models. However, irrespective of the actual mechanism that causes the isotope sensitivity, the data strongly support an assignment of the low-frequency part of the 1735 cm^{-1} vibration to the C═O stretching mode of a carboxylic acid. These arguments apply for the isotope sensitivity of peptide 1-induced bands as well. However, those bands exhibit only 20–30% of the peak intensities observed with G_t.

In the amide I region, the prominent G_t-induced band at 1640 cm^{-1} is not sensitive to H/D exchange, as shown in Fig. 6, *a–d*. For the peptide-induced changes, however, the strong 1657 cm^{-1} vibration is replaced by a pair of bands at 1657 and 1650 cm^{-1} in D_2O (Fig. 6, *e* and *f*). The amide II spectral range is also affected. A negative band at 1559 cm^{-1} becomes visible in D_2O, which may have been obscured by the amide I vibration at 1550 cm^{-1} in H_2O. This agrees well with the effect of H/D exchange on the G_t-induced bands in washed membranes and phosphatidylcholine vesicles (Fig. 6 *a*, *b* and *c*, *d*, respectively). The overlapping 1550 cm^{-1} amide II band is expected to be downshifted by 70–90 cm^{-1} in D_2O and may contribute to the positive band at 1460 cm^{-1}, which becomes enhanced in D_2O. A pronounced isotope effect is also evident for the 1517 cm^{-1} band, which in all three systems becomes reduced in D_2O.

The fact that all peptide-induced bands that correspond to G_t-induced vibrations in washed membranes or phosphatidylcholine vesicles also exhibit the same isotope sensitivity indicates that a common molecular origin is responsible for these absorptions, rather than being mere coincidence. Thus the 11 C-terminal amino acids of $G_{t\alpha}$ can effectively mimic distinct infrared spectroscopic features evoked by G_t, demonstrating that the MII-G_t interaction during light activation must be mediated mainly by the C-terminus of $G_{t\alpha}$.

Influence of amino acid replacements in the $G_{t\alpha}$ C-terminal peptide on absorption changes during MII formation

Site-directed mutagenesis of rhodopsin has proved extremely useful for band assignments in FTIR difference spectra and constitutes an important step toward an understanding of the functional role of individual amino acid side chains in receptor activation. In the case of the rhodopsin-G_t interaction, substitution of peptide 1 for G_t has been demonstrated here to preserve some characteristic spectral features of the native complex. This offers the possibility of using peptide synthesis as an alternative to mutagenesis of G_t to arrive at specific band assignments and, at the same time, to overcome limitations posed by the required amount of recombinant material in this kind of biophysical study. Amino acid replacements in peptide 1 were chosen to address the question, whether the group responsible for the 1735 cm^{-1} band in $MIIG_t$ is located on rhodopsin or G_t. For this purpose, peptide 3, i.e., peptide 1 with the replacements E342Q/D346N, was tested in the FTIR experiment. Fig. 7 *a* shows that the typical 1735 cm^{-1} band is still observed with peptide 3 and, therefore, cannot be caused by C═O stretching modes of amino acid side chains in peptide 1. In peptide 3, the free carboxy terminus has been preserved and may contribute to the 1735 cm^{-1} band as well. However, amidation of the C-terminus of peptide 3 (yielding peptide 4) does not distinctly affect the 1700–1800 cm^{-1} range during photoactivation (Fig. 7 *b*). Moreover, the amide I and II absorption changes observed with peptide 4 follow the general pattern of positive bands in the 1640–1660 cm^{-1} range and near 1550 cm^{-1}. Thus a similar interaction of the peptides with MII seems to prevail irrespective of the amino acid replacements and C-terminal amidation. Most importantly, the isotope sensitivity of the peptide 4-induced 1735 cm^{-1} band again parallels that of the $MIIG_t$ complex (Fig. 7 *c*). This strongly indicates that an identical molecular origin of the 1735 cm^{-1} mode underlies the interaction of rhodopsin with G_t and $G_{t\alpha}$ C-terminal peptides. The result

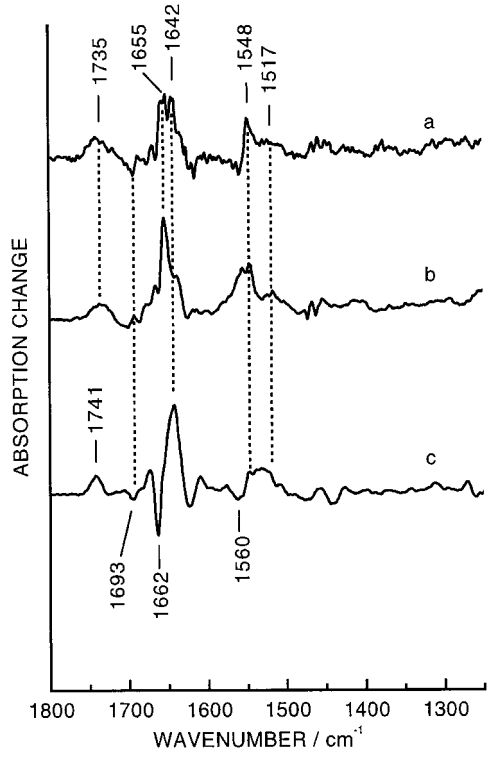

FIGURE 7 Influence of amino acid replacements on peptide-induced absorption changes during photoactivation of rhodopsin in washed membranes. (*a*) Absorption changes induced by peptide 3, i.e., peptide 1 with the replacements E342Q and D346N in H_2O. (*b* and *c*) Absorption changes induced by peptide 4, i.e., peptide 3 with amidated carboxy terminus, measured in H_2O and D_2O, respectively.

with peptide 4 excludes an involvement of the C═O groups of E342, D346, or the free carboxy terminus in absorption changes between 1770 and 1800 cm^{-1}, and agrees with the previous observation that coupling of G_t to rhodopsin is not affected by Ala substitutions for both amino acids (Garcia et al., 1995; Osawa and Weiss, 1995). Therefore, a protonated carboxyl group of rhodopsin, rather than G_t, contributes to the 1735 cm^{-1} absorption change.

CONCLUSIONS

FTIR difference spectroscopy in combination with the ATR technique allows the characterization of infrared absorption changes related to molecular recognition between biologically functional proteins and peptides. $MIIG_t$ complex formation is shown to involve mainly an interaction between the C-terminus of $G_{t\alpha}$ and MII, as shown by the reproduction of typical G_t-induced bands by residues 340–350 of $G_{t\alpha}$. D_2O and pH sensitivity in the carbonyl stretching frequency range suggest that protonation of a carboxylic acid group is stabilized during this interaction. In contrast to previous band assignments, site-directed mutagenesis could be circumvented in this study by use of $G_{t\alpha}$-derived synthetic peptides that efficiently simulate the native rhodopsin-G_t complex. In particular, the corresponding carbonyl absorption changes are preserved after the removal of carboxylic acid groups from the C-terminal $G_{t\alpha}$ peptide. This result, together with the fact that Asp^{83}, Glu^{113}, and Glu^{122} are not affected in the $MIIG_t$ complex, strongly indicates that, close to pH 7, a surface Glu or Asp of rhodopsin becomes protonated in the MII state upon binding to the $G_{t\alpha}$ C-terminus. The C-D and E-F loops of rhodopsin have been shown to provide possible binding domains for $G_{t\alpha}$ C-terminal peptides (Acharya et al., 1997). After MII formation, proton exchange reactions have been described for rhodopsin (Radding and Wald, 1965; Bennett, 1980). Heterogeneity of the MII state itself has been deduced from proton uptake studies (Arnis and Hofmann, 1993) and ascribed to different cytoplasmic surface conformations involving Glu^{134} (Arnis et al., 1994) of the cytoplasmic C-D loop as a putative proton acceptor for a pH-sensitive transition between a MII_a (unprotonated) and a MII_b (protonated) state. The participation of the conserved Glu^{134} in G_t binding and activation has been demonstrated (Cohen et al., 1993; Fahmy and Sakmar, 1993, Acharya and Karnik, 1996), and G_t has been shown to bind and thereby stabilize the MII_b state (Arnis and Hofmann, 1995). Therefore, the data agree that Glu^{134} is a prime candidate for the inferred G_t-dependent protonation event in MII and indicate that the MII structure is indeed changed upon G_t binding, as predicted by the MII_a/MII_b model. The G_t-dependent enhancement of negative bands at 1662 and 1693 cm^{-1}, already present in the normal MII difference spectrum, may also be indicative of light-induced conformational changes in rhodopsin that proceed more efficiently in the presence of G_t. Protonation of an aspartic acid residue in α_{1B}-adrenergic receptor, homologous to Glu^{134}, has been proposed (Scheer et al., 1996), but direct biophysical evidence has not yet been presented in either system. Because the rhodopsin-G_t interaction has been shown here to be functional also in reconstituted lipid vesicles and under conditions of the ATR-FTIR experiment, similar studies of reconstituted receptor mutants should allow the assignment of molecular interactions to specific amino acids of rhodopsin. Along with the simulation of protein-protein recognition by peptide-protein interactions, the ATR-FTIR technique may help to identify binding epitopes and characterize the binding mode in a variety of systems operating at the lipid-water interface.

I thank Prof. F. Siebert for having generously provided measuring facilities and for critically reading the manuscript. I am also grateful to Prof. T. P. Sakmar for his support of this work and stimulating discussions. I further thank B. Mayer for assistance in protein preparations and functional assays.

Part of this work was supported by the Deutsche Forschungsgemeinschaft (grant Fa 248/2-1).

REFERENCES

Acharya, S., and S. S. Karnik. 1996. Modulation of GDP release from transducin by the conserved Glu^{134}-Arg^{135} sequence in rhodopsin. *J. Biol. Chem.* 271:25406–25411.

Acharya, S., Y. Saad, and S. S. Karnik. 1997. Transducin-α C-terminal peptide binding site consists of C-D and E-F loops of rhodopsin. *J. Biol. Chem.* 272:6519–6524.

Arnis, S., K. Fahmy, K. P. Hofmann, and T. P. Sakmar. 1994. A conserved carboxylic acid group mediates light-dependent proton uptake and signaling by rhodopsin. *J. Biol. Chem.* 269:23879–23881.

Arnis, S., and K. P. Hofmann. 1993. Two different states of metarhodopsin II: Schiff base deprotonation precedes proton uptake and signaling state. *Proc. Natl. Acad. Sci. USA.* 90:7849–7853.

Arnis, S., and K. P. Hofmann. 1995. Photoregeneration of bovine rhodopsin from its signaling state. *Biochemistry.* 34:9333–9340.

Baenziger, J. E., K. W. Miller, and K. J. Rothschild. 1993. Fourier transform infrared difference spectroscopy of the acetylcholine receptor: evidence for specific protein structural changes upon desensitization. *Biochemistry.* 32:5448–5454.

Baldwin, J. M. 1994. Structure and function of receptors coupled to G proteins. *Curr. Opin. Cell Biol.* 6:180–190.

Bennett, N. 1980. Optical study of the light-induced changes associated with the metarhodopsin II intermediate in rod outer-segment membranes. *Eur. J. Biochem.* 111:99–103.

Bownds, D. 1967. Site of attachment of retinal in rhodopsin. *Nature.* 216:1178–1181.

Casey, P. J. 1994. Lipid modifications of G proteins. *Curr. Opin. Cell Biol.* 6:219–225.

Chabre, M. 1975. X-ray diffraction studies of retinal rods. I. Structure of the disc membrane, effect of illumination. *Biochim. Biophys. Acta.* 382:322–335.

Cohen, G. B., D. D. Oprian, and P. R. Robinson. 1992. Mechanism of activation and inactivation of opsin: role of Glu^{113} and Lys^{296}. *Biochemistry.* 31:12592–12601.

Cohen, G. B., T. Yang, P. R. Robinson, and D. D. Oprian. 1993. Constitutive activation of opsin: influence of charge at position 134 and size at position 296. *Biochemistry.* 32:6111–6115.

Coke, M., C. J. Restall, C. M. Kemp, and D. Chapman. 1986. Rotational diffusion of rhodopsin in the visual receptor membrane: effects of temperature and bleaching. *Biochemistry.* 25:513–518.

DeGrip, W. J., J. Gillespie, and K. J. Rothschild. 1985. Carboxyl group involvement in the meta I and meta II stages in rhodopsin bleaching. A Fourier transform infrared spectroscopy study. *Biochim. Biophys. Acta.* 809:97–106.

DeLange, F., M. Merkx, P. Bovee-Geurts, A. M. A. Pistorius, and W. J. DeGrip. 1997. Modulation of the metarhodopsin I/metarhodopsin II equilibrium of bovine rhodopsin by ionic strength—evidence for a surface charge effect. *Eur. J. Biochem.* 243:174–180.

Emeis, D., and K. P. Hofmann. 1981. Shift in the relation between flash-induced metarhodopsin I and metarhodopsin II within the first 10% rhodopsin bleaching in bovine disc membranes. *FEBS Lett.* 136: 201–207.

Emeis, D., H. Kühn, J. Reichert, and K. P. Hofmann. 1982. Complex formation between metarhodopsin II and GTP-binding protein in bovine photoreceptor membranes leads to a shift of the photoproduct equilibrium. *FEBS Lett.* 143:29–34.

Fahmy, K., F. Jäger, M. Beck, T. A. Zvyaga, T. P. Sakmar, and F. Siebert. 1993. Protonation states of membrane-embedded carboxylic acid groups in rhodopsin and metarhodopsin II: a Fourier-transform infrared spectroscopic study of site-directed mutants. *Proc. Natl. Acad. Sci. USA.* 90:10206–10210.

Fahmy, K., and T. P. Sakmar. 1993. Regulation of the rhodopsin-transducin interaction by a highly conserved carboxylic acid group. *Biochemistry.* 32:7229–7236.

Fung, B. K.-K., J. B. Hurley, and L. Stryer. 1981. Flow of information in the light-triggered cyclic nucleotide cascade of vision. *Proc. Natl. Acad. Sci. USA.* 75:152–156.

Ganter, U. M., E. D. Schmid, D. Perez-Sala, R. R. Rando, and F. Siebert. 1989. Removal of the 9-methyl group of retinal inhibits signal transduction in the visual process. A Fourier transform infrared and biochemical investigation. *Biochemistry.* 28:5954–5962.

Garcia, P. D., R. Onrust, S. M. Bell, T. P. Sakmar, and H. R. Bourne. 1995. Transducin-α C-terminal mutations prevent activation by rhodopsin: a new assay using recombinant proteins expressed in cultured cells. *EMBO J.* 14:4460–4469.

Gibson, N. J., and M. F. Brown. 1993. Lipid headgroup and acyl chain composition modulate the MI-MII equilibrium of rhodopsin in recombinant membranes. *Biochemistry.* 32:2438–2454.

Guy, P. M., J. G. Koland, and R. A. Cerione. 1990. Rhodopsin-stimulated activation-deactivation cycle of transducin: kinetics of the intrinsic fluorescence response of the α subunit. *Biochemistry.* 29:6954–6964.

Hadden, J. M., D. Chapman, and D. C. Lee. 1995. A comparison of infrared spectra of proteins in solution and crystalline forms. *Biochim. Biophys. Acta.* 1248:115–122.

Hamm, H. E., D. Deretic, A. Arendt, P. A. Hargrave, B. König, and K. P. Hofmann. 1988. Site of G-protein binding to rhodopsin mapped with synthetic peptides from the α subunit. *Science.* 241:832–835.

Hargrave, P. A., H. E. Hamm, and K. P. Hofmann. 1993. Interaction of rhodopsin with the G-protein, transducin. *Bio-Essays.* 15:43–50.

Hargrave, P. A., and J. H. McDowell. 1992. Rhodopsin and phototransduction: a model system for G protein-linked receptors. *FASEB J.* 6:2323–2331.

Harrick, N. J. 1967. Internal Reflection Spectroscopy. Harrick Scientific Corporation, Ossining, NY.

Harrick, N. J. 1983. Prism liquid cell. *Appl. Spectrosc.* 37:583–585.

Helmreich, E. J. M., and K. P. Hofmann. 1996. Structure and function of proteins in G-protein-coupled signal transfer. *Biochim. Biophys. Acta.* 1286:285–322.

Jäger, F., K. Fahmy, T. P. Sakmar, and F. Siebert. 1994. Identification of glutamic acid 113 as the Schiff base proton acceptor in the metarhodopsin II photointermediate of rhodopsin. *Biochemistry.* 33:10878–10882.

Kibelbek, J., D. C. Mitchell, J. M. Beach, and B. J. Litman. 1991. Functional equivalence of metarhodopsin II and the G_t-activating form of photolyzed bovine rhodopsin. *Biochemistry.* 30:6761–6768.

Klinger, A. L., and M. S. Braiman. 1992. Structural comparison of metarhodopsin II, metarhodopsin III, and opsin based on kinetic analysis of Fourier transform infrared difference spectra. *Biophys. J.* 63:1244–1255.

Kokame, K., Y. Fukada, T. Yoshizawa, T. Takao, and Y. Shimonishi. 1992. Lipid modification at the N terminus of photoreceptor G-protein α-subunit. *Nature.* 359:749–752.

König, B., A. Arendt, J. H. McDowell, M. Kahlert, P. A. Hargrave, and K. P. Hofmann. 1989a. Three cytoplasmic loops of rhodopsin interact with transducin. *Proc. Natl. Acad. Sci. USA.* 86:6878–6882.

König, B., W. Welte, and K. P. Hofmann. 1989b. Photoactivation of rhodopsin and interaction with transducin in detergent micelles. Effect of "doping" with steroid molecules. *FEBS Lett.* 257:163–166.

Krimm, S., and J. Bandekar. 1986. Vibrational spectroscopy and conformation of peptides, polypeptides, and proteins. *Adv. Protein Chem.* 38:181–365.

Kühn, H. 1980. Light- and GTP-dependent interaction of GTPase and other proteins with bovine photoreceptor membranes. *Nature.* 283:587–589.

Lewis, J. L., and D. S. Kliger. 1992. Photointermediates of visual pigments. *J. Bioenerg. Biomembr.* 24:201–210.

Liebman, P. A., and A. Sitaramayya. 1984. Role of G-protein/receptor interaction in amplified phosphodiesterase activation of retinal rods. *Adv. Cyclic Nucleotide Res.* 17:215–225.

Maeda, A., Y. J. Ohkita, J. Sasaki, Y. Shichida, and T. Yoshizawa. 1993. Water structural changes in lumirhodopsin, metarhodopsin I, and metarhodopsin II upon photolysis of bovine rhodopsin: analysis by Fourier transform infrared spectroscopy. *Biochemistry.* 32:12033–12038.

Matsuda, T., T. Takao, Y. Shimonishi, M. Murata, T. Asano, T. Yoshizawa, and Y. Fukada. 1994. Characterization of interactions between transducin alpha/beta gamma-subunits and lipid membranes. *J. Biol. Chem.* 269:30358–30363.

Nishimura, S., J. Sasaki, H. Kandori, T. Matsuda, Y. Fukada, and A. Maeda. 1996. Structural changes in the peptide backbone in complex formation between activated rhodopsin and transducin studied by FTIR spectroscopy. *Biochemistry.* 35:13267–13271.

Noel, J. P., H. E. Hamm, and P. B. Sigler. 1993. The 2.2 Å crystal structure of transducin-α complexed with GTPγS. *Nature.* 366:6544–663.

Ohkita, Y. J., J. Sasaki, A. Maeda, T. Yoshizawa, M. Groesbeek, P. Verdegem, and J. Lugtenburg. 1995. Changes in structure of the chromophore in the photochemical process of bovine rhodopsin as revealed by FTIR spectroscopy for hydrogen out-of-plane vibrations. *Biophys. Chem.* 56:71–78.

Onrust, R., P. Herzmark, P. Chi, P. D. Garcia, O. Lichtarge, C. Kingsley, and H. R. Bourne. 1997. Receptor and beta-gamma binding sites in the alpha subunit of the retinal g protein transducin. *Science.* 275:381–384.

Osawa, S., and E. R. Weiss. 1995. The effect of carboxyl-terminal mutagenesis of $G_{t\alpha}$ on rhodopsin and guanine nucleotide binding. *J. Biol. Chem.* 270:31052–31058.

Oseroff, A. R., and R. H. Callender. 1974. Resonance Raman spectroscopy of rhodopsin in retinal disk membranes. *Biochemistry.* 13:4243–4248.

Papermaster, D. S. 1982. Preparation of rod outer segments. *Methods Enzymol.* 81:48–52.

Parkes, J. H., and P. A. Liebman. 1984. Temperature and pH dependence of the metarhodopsin I-metarhodopsin II kinetics and equilibria in bovine rod disk membrane suspensions. *Biochemistry.* 23:5054–5061.

Phillips, W. J., and R. A. Cerione. 1988. The intrinsic fluorescence of the alpha subunit of transducin. Measurement of receptor-dependent guanine nucleotide exchange. *J. Biol. Chem.* 263:15498–15505.

Radding, C. M., and G. Wald. 1956. Acid-base properties of rhodopsin and opsin. *J. Gen. Physiol.* 39:909–922.

Rath, P., L. L. J. DeCaluwé, P. H. M. Boovee-Geurts, W. J. DeGrip, and K. J. Rothschild. 1993. Fourier transform infrared difference spectroscopy of rhodopsin mutants: light activation of rhodopsin causes hydrogen-bonding change in residue aspartic acid-83 during meta II formation. *Biochemistry.* 32:10277–10282.

Salamon, Z., Y. Wang, J. L. Soulages, M. F. Brown, and G. Tollin. 1996. Surface plasmon resonance spectroscopy studies of membrane proteins—transducin binding and activation by rhodopsin monitored in thin films. *Biophys. J.* 71:283–294.

Scheer, A., F. Fanelli, T. Costa, P. G. De Benedetti, and S. Cotecchia. 1996. Constitutively active mutants of the α_{1B}-adrenergic receptor—role of highly conserved polar amino acids in receptor activation. *EMBO J.* 15:3566–3578.

Schleicher, A., and K. P. Hofmann. 1987. Kinetic study on the equilibrium between membrane-bound and free photoreceptor G-protein—membrane association of G-protein. *J. Membr. Biol.* 95:271–281.

Siebert, F. 1995. Application of FTIR spectroscopy to the investigation of dark structures and photoreactions of visual pigments. *Isr. J. Chem.* 35:309–323.

Sondek, J., A. Bohm, D. G. Lambright, H. E. Hamm, and P. B. Sigler. 1996. Crystal structure of a G_A protein $\beta\gamma$ dimer at 2.1 Å resolution. *Nature.* 379:369–374.

Yoshizawa, T., and G. Wald. 1963. Pre-lumirhodopsin and the bleaching of visual pigments. *Nature.* 197:1279–1286.